



## Constrained 1-D inversion of MCSEM data on resistive oil reservoir

Luiz. Rijo & Frayzer L. Almeida, UFPA, Brazil  
rijo@amazon.com.br

Copyright 2005, SBGf - Sociedade Brasileira de Geofísica

This paper was prepared for presentation at the 9<sup>th</sup> International Congress of the Brazilian Geophysical Society held in Salvador, Brazil, 11-14 September 2005.

Contents of this paper were reviewed by the Technical Committee of the 9<sup>th</sup> International Congress of the Brazilian Geophysical Society. Ideas and concepts of the text are authors' responsibility and do not necessarily represent any position of the SBGf, its officers or members. Electronic reproduction or storage of any part of this paper for commercial purposes without the written consent of the Brazilian Geophysical Society is prohibited.

### Abstract

Recently a new and very important geophysical method for detection of oil-filled layers in deep-water areas has been introduced to the petroleum industry. The method, called Marine Controlled Source Electromagnetic (MCSEM) maps the contrast of electrical resistivity between the reservoir and the host sedimentary layers. Usually the resistivity of the former is greater than that of the latter. The method is based on the diffusion of electromagnetic energy at low frequency generated by a mobile horizontal electrical dipole and detected by an array of receivers distributed on seafloor. In this paper an efficient algorithm is proposed for inversion of 1-D MCSEM in-line electrical field data. The bathymetry and the seawater resistivity, usually knowing a priori, are used as constrains for regularization of the algorithm. The efficiency of the algorithm was tested with three models with good results. The resolution of the inversion scheme improves greatly if one uses normalized data. The information of the background resistivity distribution for the normalization process can be obtained via well logging or through MMT surveys.

### Introduction

In the last few years, a new geophysical method denominated MCSEM (Marine Controlled - Source Electromagnetic) for petroleum exploration in deep waters has drawn attention of several oil companies. The method MCSEM is based on the use of a mobile horizontal electric dipole (HED) source and an array of electric field receivers distributed on the seafloor (Eidesmo et al., 2002). The transmitting dipole emits a low frequency (0.125 to 5 Hz) signal that diffuses outwards both into the overlying water layer and downwards into the seabed sediments. The receivers at the seafloor give the amplitude and phase of the electric field signal which depends on both the geometry and resistivity of the underlying sediments. The method relies on the moderate resistivity contrast between oil-saturated reservoirs, and the surrounding sedimentary layers saturated with aqueous saline fluids.

In many cases the resistivity contrast between the oil - saturated reservoir and the surrounding sediments is very small (from 5 to 10 times greater). In this situation the detection of the reservoir is not very simple if one uses only the usual in-line  $E_x$  component of the electrical field. In this paper we discuss an algorithm for constrained 1-D

inversion using both the in-line  $E_x$  and  $E_z$  electrical field components.

### The forward problem

The equations of the in-line (radial) electrical field  $E_x$  and  $E_z$  components (SI) due to an x-oriented electrical dipole are

$$E_x^{Rad}(\bar{x}, 0, \bar{h}_1) = \frac{\rho_1 Ids}{4\pi\delta^3} \int_0^\infty K'_{TM}(g, \bar{h}_1) J_1(g\bar{x}) dg - \frac{\rho_1 Ids}{4\pi\delta^3} \int_0^\infty K'_{TM}(g, \bar{h}_1) J_0(g\bar{x}) g dg - \frac{\rho_1 Ids}{4\pi\delta^3} \int_0^\infty K_{TE}(g, \bar{h}_1) \frac{2i}{u_1} J_1(g\bar{x}) dg \quad (1)$$

where  $\rho_1$  is the resistivity of the sea-water layer and  $\delta = \sqrt{2\rho_1 / \omega\mu_0}$  is its skin-depth.  $\bar{h}_1$  is the normalized (by the skin-depth) thickness of the sea-water layer.  $\bar{x}$  is the normalized distance between the transmitter and the receiver.  $u_1 = \sqrt{g^2 + 2i}$  is the normalized propagation constant.  $J_0$  and  $J_1$  are the Bessel functions of first kind of order 0 and 1.  $Ids$  is the electrical dipole moment. Finally,  $K_{TE}$  e  $K'_{TM}$  are, respectively, the TE and TM mode kernels of the  $J_0$  and  $J_1$  Hankel transforms (see Appendix).

### The inverse problem

The proposed algorithm consist on the minimization of the objective function:

$$U(\mathbf{p}) = \sum_{k=1}^N (A_k^{obs} - A_k(E_x^{Rad}(\mathbf{p})))^2 + \sum_{k=N+1}^{2N} (F_k^{obs} - F_k(E_x^{Rad}(\mathbf{p})))^2 + l \sum_{j=1}^M (\mathbf{p}_j^* - \gamma_j)^2 \quad (2)$$

where  $\mathbf{p}$  é is the geoelectrical parameter vector (resistivity and layer thickness).  $N$  is the number of observations,  $(A_k^{obs}, F_k^{obs})$  is the vector of the amplitude and phase of the observed in-line electrical field, the vector

$(A_k(E_{x}^{Rad}(\mathbf{p})), F_k(E_{x}^{Rad}(\mathbf{p})))$  contains the theoretical in-line electrical field (Eq. 1),  $\ell$  is the Lagrange's multiplier,  $M$  is the number of constrained parameters,  $\mathbf{p}^*$  is the constrained parameter vector and finally,  $\gamma$  is the vector with the absolute constrained parameter values. The inversion algorithm is based on Marquardt's strategy using the scheme proposed by Medeiros & Silva (1996) and Luiz (1999).

**Examples**

In order to illustrate the performance of our inversion algorithm we show here three examples. The first one, called Model A, represents a thick (100 m) and very resistive reservoir (100 ohm-m), located 1000m beneath the sea floor, as shown in Table 1. The sea layer is 800 m thick with seawater resistivity equal to 0.3 ohm-m. The frequency of the HED transmitter is 0.5 Hz. This model was suggested by Eidesmo et al. 2002 and, unfortunately, is not realistic for Brazilian platform. The other two models (Model B and C) suggested by Marco Polo (personal communication) are much more realistic in Brazil. The reservoir layer is thinner (50 m) and much less resistive (10 ohm-m). In the model B the reservoir layer is located 1500 m beneath the sea floor whereas in model C it is located at 2450 m. In these models the sea layer has 1500 m of thickness and the frequency of the HED transmitter is 0.125 Hz.

**Modelo A**

Synthetic data with 5% noise were calculated using the information on Table 1 to simulate observed data for the model A. The seawater resistivity and sea layer thickness ( $\rho_1$  and  $h_1$ ) are supposed to be known and also the resistivity of underlying sediments ( $\rho_2$ ). These parameters were used as absolute constrains to estimate the resistivity and thickness of the reservoir layer ( $\rho_3$  and  $h_3$ ) and the depth  $h_2$ . The first guess model is illustrated in Table 2.

| Model A                        |                          |
|--------------------------------|--------------------------|
| $\rho_1 = 0.3 \text{ ohm-m}$   | $h_1 = 800.0 \text{ m}$  |
| $\rho_2 = 1.0 \text{ ohm-m}$   | $h_2 = 1000.0 \text{ m}$ |
| $\rho_3 = 100.0 \text{ ohm-m}$ | $h_3 = 100.0 \text{ m}$  |
| $\rho_4 = 1.0 \text{ ohm-m}$   |                          |

Table 1: The parameters in red are the absolute constrained parameters.

| First guess                    |                          |
|--------------------------------|--------------------------|
| $\rho_1 = 0.33 \text{ ohm-m}$  | $h_1 = 800.0 \text{ m}$  |
| $\rho_2 = 1.20 \text{ ohm-m}$  | $h_2 = 1500.0 \text{ m}$ |
| $\rho_3 = 200.0 \text{ ohm-m}$ | $h_3 = 150.0 \text{ m}$  |
| $\rho_4 = 1.30 \text{ ohm-m}$  |                          |

Table 2: The first guess for the model A.

After 40 iterations it was obtained the model shown in Table 3, illustrated graphically on Figure 1. Note that the estimated model is very closed to the model used for generating the "observed" data. Figure 2 shows the amplitude and phase of the estimated model compared with the "observed" data.

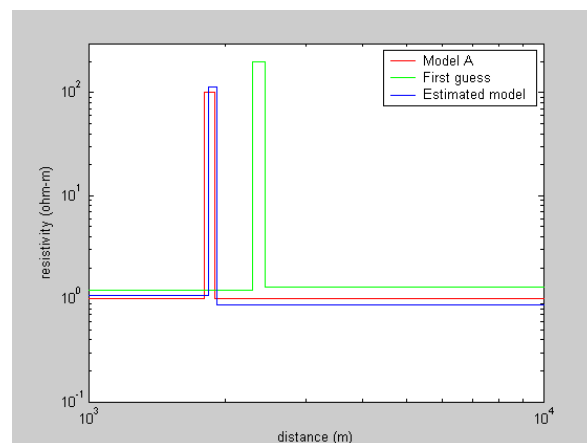


Figure 1: Graphic representation of the Table 3.

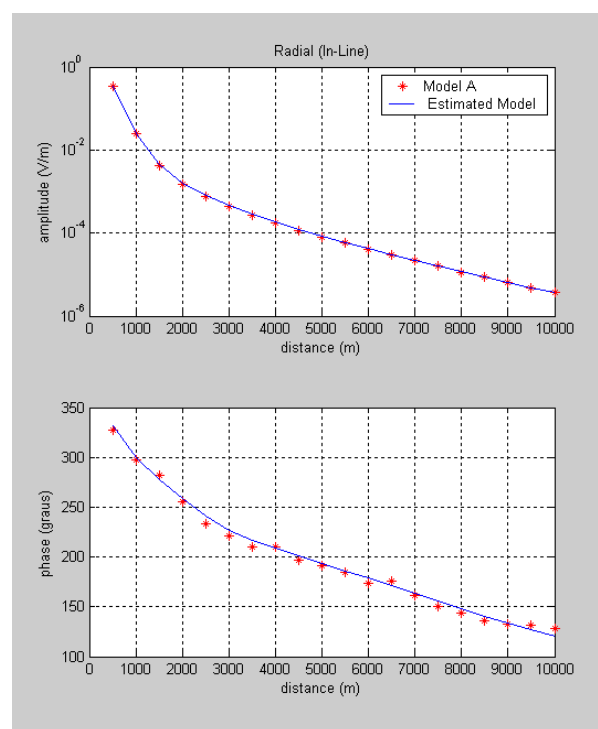


Figure 2: Comparison of the amplitude and phase of the in-line electrical field normalized by  $I_{ds} / 4\pi\delta^3$  of the estimated model and the "observed" data.  $f = 0.5 \text{ Hz}$ .

| Estimated model            |                       |
|----------------------------|-----------------------|
| <b>rho1 = 0.30 ohm-m</b>   | <b>h1 = 835.15 m</b>  |
| <b>rho2 = 1.07 ohm-m</b>   | <b>h2 = 1000.38 m</b> |
| <b>rho3 = 113.63 ohm-m</b> | <b>h3 = 84.02 m</b>   |
| <b>rho4 = 0.88 ohm-m</b>   |                       |

Table 3: The estimated parameters of Model A.

**Model B**

Synthetic data with 5% noise were calculated using the information on Table 4 to simulate observed data for the model B. The seawater resistivity and sea layer thickness (rho1 and h1) are supposed to be known and also the resistivity of underlying sediments (rho2). These parameters were used as absolute constrains to estimate the resistivity and thickness of the reservoir layer (rho3 and h3) and the depth h2. The first guess model is illustrated in Table 5.

| Model B                  |                      |
|--------------------------|----------------------|
| <b>rho1 = 0.3 ohm-m</b>  | <b>h1 = 1500.0 m</b> |
| <b>rho2 = 0.8 ohm-m</b>  | <b>h2 = 1000.0 m</b> |
| <b>rho3 = 10.0 ohm-m</b> | <b>h3 = 50.0 m</b>   |
| <b>rho4 = 0.8 ohm-m</b>  |                      |

Table 4: The parameters in red are the absolute constrained parameters.

| First guess              |                      |
|--------------------------|----------------------|
| <b>rho1 = 0.33 ohm-m</b> | <b>h1 = 1500.0 m</b> |
| <b>rho2 = 0.89 ohm-m</b> | <b>h2 = 1300.0 m</b> |
| <b>rho3 = 40.0 ohm-m</b> | <b>h3 = 80.0 m</b>   |
| <b>rho4 = 0.98 ohm-m</b> |                      |

Table 5: The first guess for the model B.

| Estimated model          |                    |
|--------------------------|--------------------|
| <b>rho1 = 0.28 ohm-m</b> | <b>h1 = 1502 m</b> |
| <b>rho2 = 0.81 ohm-m</b> | <b>h2 = 1094 m</b> |
| <b>rho3 = 12.5 ohm-m</b> | <b>h3 = 35 m</b>   |
| <b>rho4 = 0.48 ohm-m</b> |                    |

Table 6: The estimated parameters of Model A.

After 40 iterations it was obtained the model shown in Table 7, illustrated graphically on Figure 3. Note that the estimated model is very closed to the model used for generating the “observed” data. Figures 4 shows the amplitude and phase of the estimated model compared with the “observed” data. Although this model is more difficult than the model A, the inversion results were equally good.

**Model C**

Synthetic data with 5% noise were calculated using the information on Table 7 to simulate observed data for the model C.

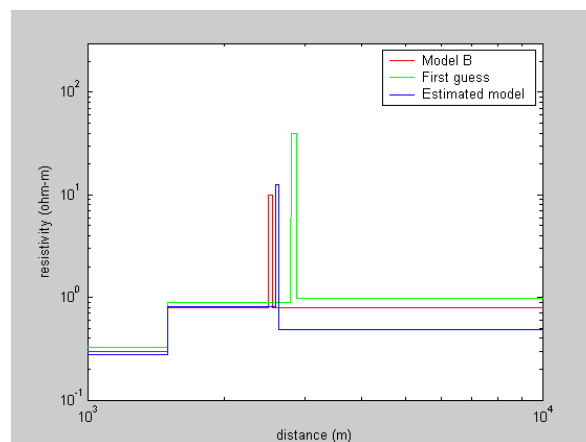


Figure3: Graphic representation of the Table 6.

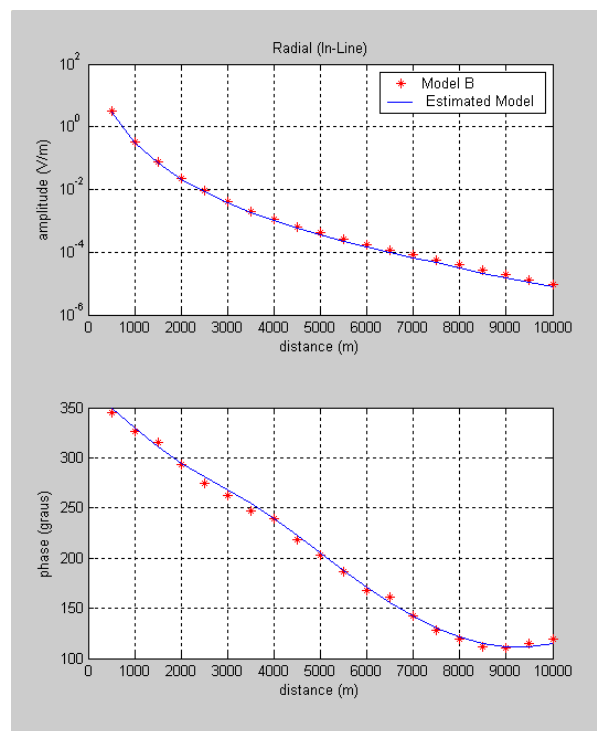


Figure 4: Comparison of the amplitude and phase of the in-line electrical field normalized by  $Ids / 4\pi\delta^3$  of the estimated model and the “observed” data  $f = 0.125$  Hz.

The seawater resistivity and sea layer thickness (rho1 and h1) are supposed to be known and also the resistivity of underlying sediments (rho2). These parameters were used as absolute constrains to estimate the resistivity and

thickness of the reservoir layer (rho3 and h3) and the depth h2. The first guess model is illustrated in Table 8.

| Model C           |               |
|-------------------|---------------|
| rho1 = 0.3 ohm-m  | h1 = 1500.0 m |
| rho2 = 0.8 ohm-m  | h2 = 2450.0 m |
| rho3 = 10.0 ohm-m | h3 = 50.0 m   |
| rho4 = 0.8 ohm-m  |               |

Table 7: The parameters in red are the absolute constrained parameters.

| First guess       |               |
|-------------------|---------------|
| rho1 = 0.30 ohm-m | h1 = 1500.0 m |
| rho2 = 0.80 ohm-m | h2 = 2000.0 m |
| rho3 = 40.0 ohm-m | h3 = 90.0 m   |
| rho4 = 0.80 ohm-m |               |

Table 8: The first guess for the model B.

| Estimated model   |              |
|-------------------|--------------|
| rho1 = 0.30 ohm-m | h1 = 1510. m |
| rho2 = 0.72 ohm-m | h2 = 2141 m  |
| rho3 = 30.5 ohm-m | h3 = 70 m    |
| rho4 = 1.2 ohm-m  |              |

Table 9: The estimated parameters of Model A.

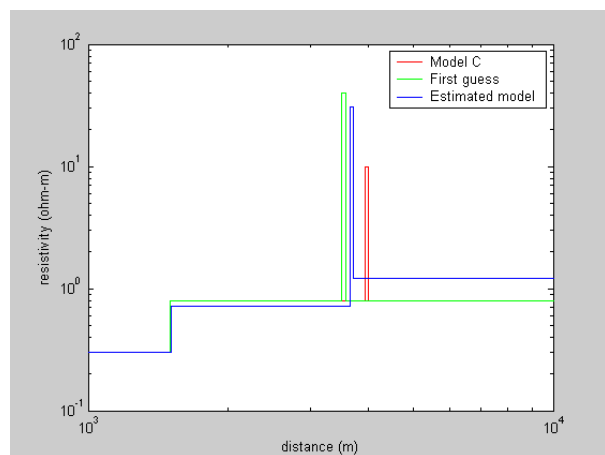


Figure 5: Graphic representation of the Table 6.

As shown in Figure 5 the estimation of Model C is not as good as the estimation of the two previous models. In all three models the estimated resistivity of the sediments above and below the reservoir layer is lightly different.

A practical expedient using in the interpretation of MCSEM data is to normalize the components of the observed electrical field by those from a background without the oil reservoir.

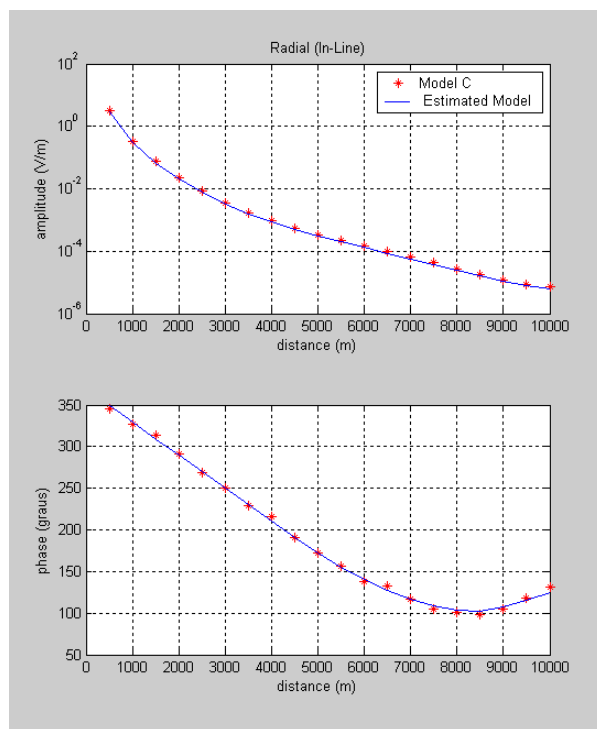


Figure 6: Comparison of the amplitude and phase of the in-line electrical field normalized by  $Ids / 4\pi\delta^3$  of the estimated model and the “observed” data  $f = 0.125$  Hz.

Using normalize data the inversion process improves substantially. This can be attested observing the Illustrations 5, 6 and 7 corresponding to the models A, B and C, respectively. Here, the same first guess models (Table 2, 5 and 8) were used for each corresponding case. The number of iteration was practically the same as before. Now, the estimate resistivity values above and below the reservoir layer are identical as they should be.

The normalization of the observed data (with the oil reservoir) by the background data (without the oil reservoir) can be considered as a kind of constrains that stabilized the inversion algorithm, given better-estimated parameter results.

**Conclusions**

MCSEM is a new geophysical method for mapping resistive layers associated with t well knows that inversion of geophysical data is a mathematical ill posed problem. Without constrains it is impossible to invert real geophysical data. MCSEM 1-D data can be constrained easily, since the resistivity of the seawater and the bathymetry of the seafloor are usually known a priori. Also, the resistivity of the sediments below the seafloor can be estimated by electrical well logging or by MMT surveys. In this paper it was shown by mean of three examples that these kind of parameter constrains is fairly effective for estimating the oil reservoir parameter (resistivity, thickness and depth). The effectiveness of the parameter estimation increases substantially if one uses normalized data. The proposed inversion algorithm can

be easily applied to the azimuthal (broad-side)  $E_x$  component data.

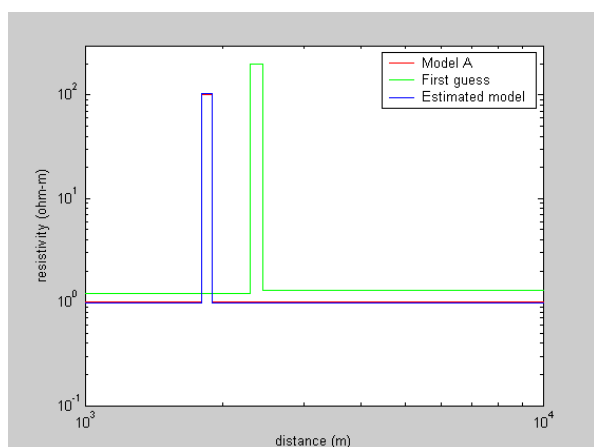


Figure 7: Graphic of the inversion result of Model A with normalized data.

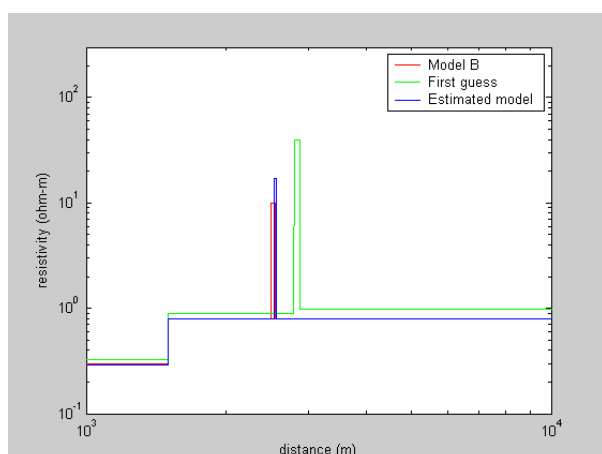


Figure 8: Graphic of the inversion result of Model B with normalized data.

### Acknowledgments

The authors acknowledge the support of Petrobrás (Contract Petrobras/Fadsp/UFPA 6502282033). L. Rijo acknowledges the ANP PRH-06 for his PV fellowship and also for supporting the PROEM Laboratory. Especial thanks are given to Dr. Marco Polo from Petrobras for many hours of fruitful discussion on MCSEM method.

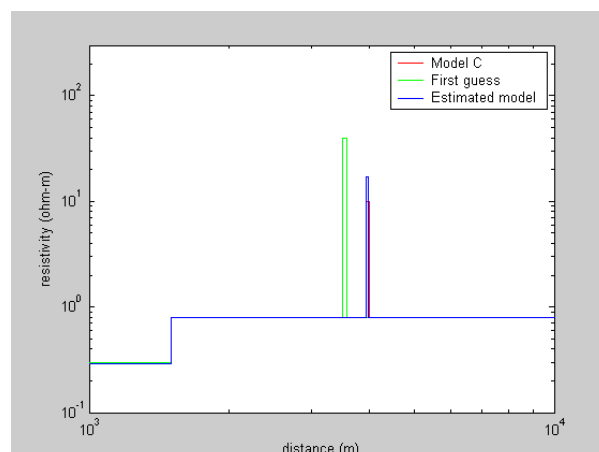


Figure 9: Graphic of the inversion result of Model C with normalized data.

### References

EIDESMO, T., ELLINGSRUD, S., MACGREGOR, L. M., CONSTABLE, SINHA, M. C., JOHANSEN, S., KONG, F. N. and WESTERDAHL, H., 2002. Sea Bed Logging (SBL), a new method for remote and direct identification of hydrocarbon filled layers in deepwater areas: First Break, 20, 144 – 152.

LUIZ, J. G 1999. Informação a priori na inversão de dados Magnetotelúricos. Tese de Doutorado, UFPA. 92 p.

MEDEIROS, W. E & SILVA J. B. C. ,1996. Geophysical inversion using approximate equality constrains. Geophysics, , 61, 1678 – 1688.

### Appendix

The  $K_{TE}$  e  $K_{TM}$  kernels of the Hank transform (1) are given by

$$\bar{K}'_{TM}(g, z) = \bar{u}_1 \left( 1 + R_{TM}^{(1)-} - R_{TM}^{(1)+} \right) e^{-\bar{u}_1(\bar{h}_1 - h_0)}$$

$$K_{TE}(g, z) = \frac{2i}{\bar{u}_1} \left( 1 + R_{TE}^{(1)-} + R_{TE}^{(1)+} \right) e^{-\bar{u}_1(\bar{h}_1 - h_0)}$$

where the reflection coefficients  $R_{TM}^{(1)-}$ ,  $R_{TM}^{(1)+}$ ,  $R_{TE}^{(1)-}$ ,  $R_{TE}^{(1)+}$  are expressed by

$$R_{TM}^{(1)-} = \frac{e^{-2\bar{u}_1\bar{h}_0} - \frac{\rho_1\bar{u}_1 - \rho_2\bar{u}_2 F_{TM}^{(2)}}{\rho_1\bar{u}_1 + \rho_2\bar{u}_2 F_{TM}^{(2)}} e^{-2\bar{u}_1\bar{h}_1}}{1 + \frac{\rho_1\bar{u}_1 - \rho_2\bar{u}_2 F_{TM}^{(2)}}{\rho_1\bar{u}_1 + \rho_2\bar{u}_2 F_{TM}^{(2)}} e^{-2\bar{u}_1\bar{h}_1}}$$

$$R_{TM}^{(1)+} = \frac{\frac{\rho_1 \bar{u}_1 - \rho_2 \bar{u}_2 F_{TM}^{(2)}}{\rho_1 \bar{u}_1 + \rho_2 \bar{u}_2 F_{TM}^{(2)}} \left( 1 + e^{-2\bar{u}_1 \bar{h}_0} \right)}{1 + \frac{\rho_1 \bar{u}_1 - \rho_2 \bar{u}_2 F_{TM}^{(2)}}{\rho_1 \bar{u}_1 + \rho_2 \bar{u}_2 F_{TM}^{(2)}} e^{-2\bar{u}_1 \bar{h}_1}},$$

$$\bar{R}_{TE}^{(1)-} = \frac{\frac{\bar{u}_1 - g}{\bar{u}_1 + g} \left[ e^{-2\bar{u}_1 \bar{h}_0} + \frac{\bar{u}_1 - \bar{u}_2 F_{TE}^{(2)}}{\bar{u}_1 + \bar{u}_2 F_{TE}^{(2)}} e^{-2\bar{u}_1 \bar{h}_1} \right]}{1 - \frac{\bar{u}_1 - g}{\bar{u}_1 + g} \left( \frac{\bar{u}_1 - \bar{u}_2 F_{TE}^{(2)}}{\bar{u}_1 + \bar{u}_2 F_{TE}^{(2)}} \right) e^{-2\bar{u}_1 \bar{h}_1}},$$

$$\bar{R}_{TE}^{(1)+} = \frac{\frac{\bar{u}_1 - \bar{u}_2 F_{TE}^{(2)}}{\bar{u}_1 + \bar{u}_2 F_{TE}^{(2)}} \left( 1 + \frac{\bar{u}_1 - g}{\bar{u}_1 + g} e^{-2\bar{u}_1 \bar{h}_0} \right)}{1 - \frac{\bar{u}_1 - g}{\bar{u}_1 + g} \left( \frac{\bar{u}_1 - \bar{u}_2 F_{TE}^{(2)}}{\bar{u}_1 + \bar{u}_2 F_{TE}^{(2)}} \right) e^{-2\bar{u}_1 \bar{h}_1}}.$$

The layering coefficient  $F_{TM}^{(2)}$  and  $F_{TE}^{(2)}$  are calculated recursively by

$$F_{TM}^{(N)} = 1,$$

$$F_{TM}^{(j)} = \frac{\rho_{j+1} \bar{u}_{j+1} F_{TM}^{(j+1)} + \rho_j \bar{u}_j \tanh \bar{u}_j \bar{h}_j}{\rho_j \bar{u}_j + \rho_{j+1} \bar{u}_{j+1} F_{TM}^{(j+1)} \tanh \bar{u}_j \bar{h}_j}, \quad j = N-1, N-2, \dots, 3, 2,$$

and

$$F_{TE}^{(N)} = 1,$$

$$F_{TE}^{(j)} = \frac{\bar{u}_{j+1} F_{TE}^{(j+1)} + \bar{u}_j \tanh \bar{u}_j \bar{h}_j}{\bar{u}_j + \bar{u}_{j+1} F_{TE}^{(j+1)} \tanh \bar{u}_j \bar{h}_j}, \quad j = N-1, N-2, \dots, 3, 2.$$